Regular Article

THROMBOSIS AND HEMOSTASIS

Targeted mutagenesis of zebrafish antithrombin III triggers disseminated intravascular coagulation and thrombosis, revealing insight into function

Yang Liu,[1] Colin A. Kretz,[2] Morgan L. Maeder,[3] Catherine E. Richter,[1] Philip Tsao,[1] Andy H. Vo,[1] Michael C. Huarng,[1] Thomas Rode,[1] Zhilian Hu,[1] Rohit Mehra,[4] Steven T. Olson,[5] J. Keith Joung,[3,6] and Jordan A. Shavit[1,7]

[1]Department of Pediatrics and [2]Life Sciences Institute, University of Michigan, Ann Arbor, MI; [3]Molecular Pathology Unit, Massachusetts General Hospital, Charlestown, MA; [4]Department of Pathology, University of Michigan, Ann Arbor, MI; [5]Center for Molecular Biology of Oral Diseases, University of Illinois, Chicago, IL; [6]Department of Pathology, Harvard Medical School, Boston, MA; and [7]Cellular and Molecular Biology Program, University of Michigan, Ann Arbor, MI

Key Points

- Juvenile zebrafish tolerate widespread coagulopathy due to complete ablation of antithrombin III, but develop lethal thrombosis as adults.

- In vivo structure/function analysis of antithrombin III in zebrafish reveals limited roles for heparin-binding and anti-IXa/Xa activity.

Pathologic blood clotting is a leading cause of morbidity and mortality in the developed world, underlying deep vein thrombosis, myocardial infarction, and stroke. Genetic predisposition to thrombosis is still poorly understood, and we hypothesize that there are many additional risk alleles and modifying factors remaining to be discovered. Mammalian models have contributed to our understanding of thrombosis, but are low throughput and costly. We have turned to the zebrafish, a tool for high-throughput genetic analysis. Using zinc finger nucleases, we show that disruption of the zebrafish antithrombin III (at3) locus results in spontaneous venous thrombosis in larvae. Although homozygous mutants survive into early adulthood, they eventually succumb to massive intracardiac thrombosis. Characterization of null fish revealed disseminated intravascular coagulation in larvae secondary to unopposed thrombin activity and fibrinogen consumption, which could be rescued by both human and zebrafish at3 complementary DNAs. Mutation of the human AT3-reactive center loop abolished the ability to rescue, but the heparin-binding site was dispensable. These results demonstrate overall conservation of AT3 function in zebrafish, but reveal developmental variances in the ability to tolerate excessive clot formation. The accessibility of early zebrafish development will provide unique methods for dissection of the underlying mechanisms of thrombosis. (*Blood*. 2014;124(1):142-150)

Introduction

Venous thrombosis affects approximately 1 in 1000 individuals, resulting in over 300 000 hospitalizations per year. There are many well-described coagulation factor defects which are associated with thrombosis, including deficiencies of the natural anticoagulant proteins, protein C (PROC), protein S (PROS1), and antithrombin III (AT3).[1] Homozygous deficiency of PROC or PROS1 is exceedingly rare and results in neonatal purpura fulminans in humans.[1] However, mouse knockout models display more severe phenotypes, with neonatal and embryonic loss for PROC and PROS1 deficiency, respectively.[2-4] Complete loss of AT3 has not been described in humans, and is presumed to be in utero lethal.[1] This is supported by the observation that homozygous deletion of AT3 in mice results in prenatal lethality, with widespread fibrin deposition in the heart and liver.[5] AT3-deficient embryos also exhibit paradoxical hemorrhage, suggesting a consumptive coagulopathy,[5] but this has been difficult to study given the relative inaccessibility of mammalian embryogenesis.

AT3 (also known as SERPINC1) is a serpin (serine protease inhibitor) that regulates many coagulation proteases including thrombin and factors IXa and Xa,[6,7] and consists of 2 functional domains. The reactive center loop (RCL) presents the Arg393-Ser394 bond for cleavage, resulting in the formation of a stable inactive AT3-protease complex. The heparin-binding site binds endogenous glycosaminoglycans or infused heparin, acting as a bridge to the protease and inducing allosteric changes in AT3, which accelerates inhibition.[6,7] Deficiency of AT3 is classified into 2 categories: type I with reduced plasma antigen levels and type II with functional defects, but normal AT3 levels.[1] The latter is further subdivided into reactive site, heparin binding, and pleiotropic defects. Over 200 different mutations from patients with AT3 deficiency have been identified,[8] and rapid advances in sequencing technologies guarantee that there are many more to come. Although in vitro assays are available for assessment of AT3 function, in some patients the underlying mechanism of AT3 deficiency remains unknown.

Teleost fish possess highly conserved orthologs of nearly all blood coagulation factors.[9-12] Zebrafish (*Danio rerio*) have been widely used to study hemostasis, demonstrating conservation and function of the structural components of coagulation, including

Figure 1. Targeted disruption of *at3* using genome editing nucleases results in adult lethality. (A) ZFN-induced deletions in somatic cells. Of 16 pooled morphologically normal embryos from 2 individual experiments, 3 of 192 sequences were identified with Δ5 (2x) and Δ9 (1x) in exon 5. The top line is the *at3* reference genome sequence from an unrelated individual. The blue and green arrows indicate 5' and 3' ZFN-binding sites, respectively. Deletions are indicated by red dashes. (B) Sequences of ZFN-induced mutations transmitted through the germline. Red dashes and letters indicate deletions and insertions, respectively. (C) Survival curve of a total of 3 clutches derived from *at3*Δ90 heterozygous incrosses shows loss of homozygotes. Offspring were genotyped at 2 to 4 months of age and tracked over 1 year. The results demonstrate a highly significant difference in the survival of homozygous mutants by log-rank (Mantel-Cox) analysis ($P < .0001$). (D) Externally visible secondary hemorrhage in an *at3*Δ90 homozygous mutant is indicated by an arrow. This fish was identified while alive, anesthetized, and the image was captured using a Leica MZ16FA microscope and a Canon EOS60D camera. (E-F) RT-PCR analysis of *at3*Δ90 mutants demonstrates reduction of *at3* expression in heterozygotes and absence of homozygous mutant mRNA. (E) Top: Total mRNA was prepared from adult fish (4 mpf) followed by qualitative RT-PCR. Bottom: Genotyping of *at3*Δ90 mutants. (F) Total mRNA was prepared from pooled larvae (3 dpf, n = 15 for each genotype) followed by quantitative real-time PCR. Error bars represent standard deviation and statistical significance was determined by *t* test. (G) *at3*Δ22 homozygous mutants were injected with a *ubi* regulated *at3* cDNA expression vector and followed for 1 year.
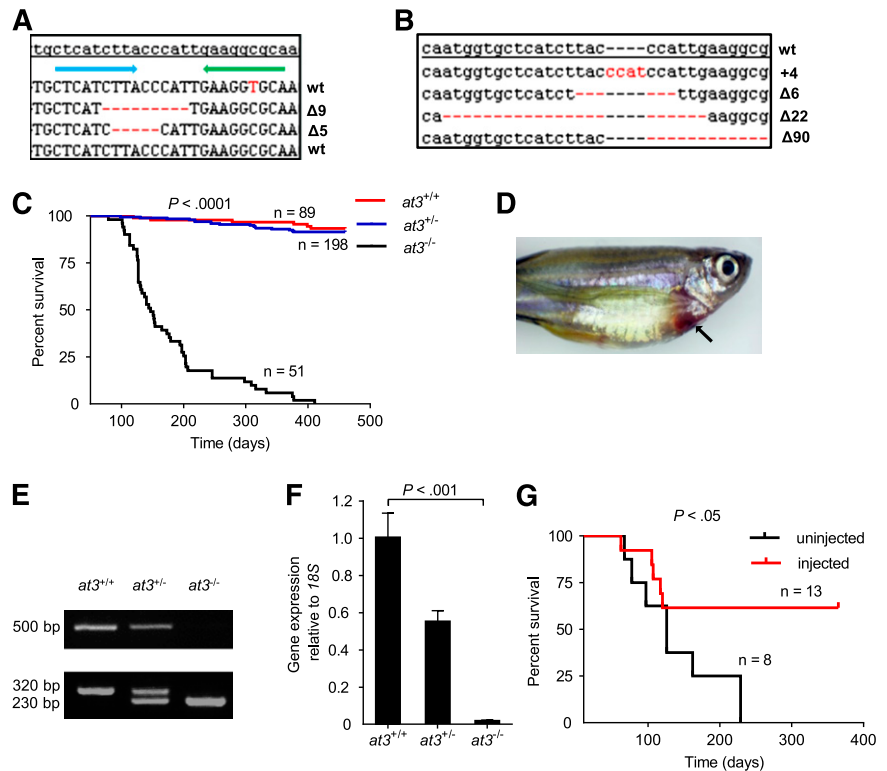
fibrinogen[13,14] and von Willebrand factor,[15,16] and the ability to develop thrombosis in response to a laser-induced injury.[14,17] Embryonic development is external, rapid, and transparent, allowing unfettered access to studies of the circulatory system. Individual breeding pairs can produce hundreds of offspring with each pairing, facilitating high-throughput genetic and small-molecule screens.[18]

Recent advances in genome editing technologies have enabled robust platforms for genetic modification.[19-21] We now report ablation of *at3* using zinc finger (ZF) nucleases (ZFNs). Although homozygous mutants recapitulate the consumptive coagulopathy and thrombotic phenotypes of the mouse knockout, the timing demonstrates significant differences. *at3*$^{-/-}$ zebrafish are able to tolerate spontaneous thrombosis and rampant disseminated intravascular coagulation (DIC) early in development, but die in adulthood with associated intracardiac thrombosis. Furthermore, using in vivo genetic complementation, we reveal insight into the hemostatic consequences of human AT3 variants.

Methods

Animals

Zebrafish were raised in accordance with animal care guidelines as approved by the University of Michigan Animal Care and Use Committee. Embryos are defined as 0 to 2 days postfertilization (dpf), and larvae as 3 to 29 dpf.

Targeted mutagenesis using ZFNs

ZFN pairs were designed to target exon 5 of the *at3* genomic locus. ZF arrays were constructed using OPEN (Oligomerized Pool ENgineering) as described.[22,23] Targeted mutagenesis with the constructed ZFNs was completed essentially as described.[19,24] ZF arrays were cloned into expression vectors

pMLM290 and 292, and transcribed in vitro using T7 mMESSAGE mMACHINE (Ambion). One nanogram of each left and right ZFN messenger RNA (mRNA) was injected into 1-cell AB × TL F1 embryos, as described.[14] At 2 to 3 dpf, 8 morphologically normal embryos were pooled and lysed in buffer (10 mM Tris, pH 8.0, 200 mM NaCl, 10 mM EDTA, 0.5% sodium dodecyl sulfate [SDS], 100 μg/mL Proteinase K) at 50°C for 2 to 3 hours, and genomic DNA isolated by phenol:chloroform extraction and ethanol precipitation. Polymerase chain reaction (PCR) of the target site was performed, and products cloned into pCR-Blunt (Invitrogen). PCR of 96 colonies was performed using M13 reverse and T7 primers, and products sequenced. The remaining injected F0 embryos were raised to adulthood and crossed to wild-type fish. Sixteen to 24 F1 embryos from each F0 founder were screened for ZFN-induced mutations by PCR of the target site with a 6-FAM–labeled gene-specific primer, after lysis in PCR extraction buffer[24] (10 mM Tris pH 8.0, 2 mM EDTA, 0.2% Triton X-100 and 100 μg/mL Proteinase K). PCR products were resolved by capillary electrophoresis on a 3730XL DNA Analyzer (Applied Biosystems). Data were processed using GeneMarker (Softgenetics LLC) for mutant identification. The remaining F1 offspring were raised to adulthood and heterozygotes identified by fin clip genotyping.

Genotyping of mutant offspring

Fin clip biopsies were obtained from adult fish after anesthesia in tricaine (0.16 mg/mL; Western Chemical Inc), and larvae were humanely killed in high-dose tricaine (1.6 mg/mL), followed by lysis in PCR extraction buffer.[24] Deletion mutations were detected by PCR and agarose gel electrophoresis (Figure 1E bottom). Primers were designed using Primer3[25] and oligonucleotides ordered from Integrated DNA Technologies. All oligonucleotide sequences are listed in supplemental Tables 1-2 (see supplemental Data available on the *Blood* Web site).

Construction of *at3* in vivo expression vectors

Vectors pubi-zat3-EGFP and pubi-hAT3-EGFP were constructed by inserting complementary DNA (cDNA) sequences under control of the *ubi* promoter in

frame with enhanced green fluorescent protein (*EGFP*) in pDestTol2pA2_ubi:EGFP[26] (supplemental Figure 1). Zebrafish *at3* was amplified from total adult cDNA using *Nco*I tagged primers, and cloned into *Nco*I digested pDestTol2-pA2_ubi:EGFP. Human *AT3* was amplified from liver cDNA using primers designed for sequence- and ligation-independent cloning, and cloned into *Nco*I digested pDestTol2pA2_ubi:EGFP as described.[27]

Zebrafish and human *at3* substitutions were introduced into pubi-zat3-EGFP and pubi-hAT3-EGFP, respectively, as described with some modifications.[28] Mutagenic primers amplified the plasmids using Phusion DNA polymerase (New England Biolabs) as follows: 98°C for 3 minutes; 4 cycles of 98°C for 10 seconds, 55°C for 30 seconds, 72°C for 8 minutes; 12 cycles of 98°C for 10 seconds, 60°C for 30 seconds, 72°C 8 minutes; 72°C for 10 minutes. PCR products were column purified, digested with *Dpn*I, and transformed into TOP10 cells, and mutations confirmed by sequencing. Amino acid numbering of human AT3 begins at +1 after the propeptide cleavage site (amino acid 33 from the initiation methionine), reflecting absence of the 32-aa propeptide. The N-terminal amino acids of zebrafish At3 are not conserved with the mammalian AT3 propeptide (supplemental Figure 2), therefore, +1 for the former is from the initiation methionine.

One-cell injection of *at3* expression vectors

Circular *at3* expression plasmids (25 ng/μL) and transposase mRNA (25 ng/μL)[29] were coinjected into 1-cell stage embryos from $at3^{\Delta90}$ or $at3^{\Delta22}$ heterozygous incrosses. Fluorescent embryos were raised to adulthood or selected for laser-mediated endothelial injury.

In vitro binding studies

Zebrafish *at3* cDNA was cloned into the *Bam*HI site of pcDNA3.1V5/HIS (Invitrogen) to produce pcDNA3.1-zat3. HEK 293 cells were grown in Dulbecco's Modified Eagle Medium (DMEM) supplemented with 10% fetal bovine serum at 37°C in 5% CO_2. The cells were transiently transfected with pcDNA3.1-zat3 using polyethylenimine (Sigma-Aldrich), incubated in serum-free DMEM for 36 hours, and lysed in 50 mM Tris-HCl (pH 8.0), 150 mM NaCl, 2 mM EDTA, and 0.5% Nonidet P40. Recombinant protein was purified using anti-V5 beads (Invitrogen), mixed with 10 μg of human thrombin (Sigma-Aldrich), incubated at 4°C for 2 hours, and washed 4 times with lysis buffer. Cell lysates and beads were boiled and separated on a 4% to 20% SDS–polyacrylamide gel electrophoresis (SDS-PAGE) gel (Bio-Rad). Western blotting was performed using anti-human thrombin antibody (Affinity Biologicals) as described in the next section.

Adult blood collection and western blotting

Adult fish blood was collected in EDTA-coated microcapillary tubes (Drew Scientific Inc) as described (see supplemental Methods for a detailed description).[30,31] Plasma was obtained by centrifugation at 1000*g* for 10 minutes at room temperature, and stored at −80°C. Two microliters from pooled wild-type or $at3^{\Delta90/\Delta90}$ fish were boiled for 5 minutes in sample buffer (Bio-Rad) and β-mercaptoethanol (Sigma-Aldrich), resolved on 4% to 20% SDS-PAGE gels, and transferred to nitrocellulose membranes (Bio-Rad). Membranes were blocked in 5% nonfat milk in 1% Triton in Tris-buffered saline at 4°C overnight and incubated with zebrafish anti-fibrinogen antibody for 1 hour at room temperature, washed, incubated with horseradish peroxidase–conjugated secondary antibody (Santa Cruz Biotechnology), washed again, and developed with chemiluminescent substrate (Super-Signal West Femto; Thermo-Scientific), and scanned with FluorChem (ProteinSimple).

In situ hybridization

RNA in situ hybridization was carried out as described.[32] Probes were generated from total zebrafish cDNA using primers with SP6 and T7 overhangs, followed by in vitro transcription with digoxygenin-labeled nucleotides.

Thrombin injection

Four milliunits of bovine thrombin (Sigma-Aldrich) were retro-orbitally infused[33] into 4 dpf larvae from $at3^{\Delta90/+}$ intercrosses. Phenotypes were collected 2 minutes postinjection by observers blinded to genotype. After phenotyping, larvae were lysed and genotyped (see supplemental Methods for a detailed description).

Laser-mediated endothelial injury

Endothelial injury was executed using a pulsed nitrogen dye laser and focusing system (MicroPoint; Andor Technology) as described.[14,17] Larvae (3-4 dpf) were anesthetized in tricaine, embedded in 0.8% low-melt agarose on glass cover slips, and visualized on an inverted microscope (Olympus IX71, 40× objective). The posterior cardinal vein (PCV) endothelium was targeted and laser-ablated at the fifth somite distal from the anal pore at power level 18 using 100 pulses. The time to occlusion was recorded up to 2 minutes. Larvae were recovered from agarose and genotyped.

Fibrinogen injection and ε-aminocaproic acid treatment

Offspring from $at3^{\Delta90/+}$ and $at3^{\Delta90/\Delta90}$ crosses were either infused with 50 ng (2 nL) human fibrinogen or bovine serum albumin (Sigma-Aldrich) in saline at 3 dpf, or preincubated with 0.1M ε-aminocaproic acid at 2 dpf, and laser injury performed at 60 minutes postinjection or 24 hours postincubation, respectively, followed by genotyping.

FITC-fibrinogen labeling and infusion

Human fibrinogen was labeled with fluorescein isothiocyanate (FITC; Thermo-Scientific), PD-10 column purified, and dye-to-protein molar ratio determined by manufacturer's instructions. Eight to 20 ng of a 1:1 molar ratio of FITC:fibrinogen was infused at 3 dpf.

Embryos were incubated in 50 μg/mL warfarin (Sigma-Aldrich) for 48 hours prior to FITC-fibrinogen infusion, or larvae infused with 1 mg/mL tissue plasminogen activator (tPA; Alteplase) via retro-orbital injection. At 3 dpf, larvae were infused with FITC-fibrinogen and evaluated 1 hour postinjection or postinfusion with tPA, and images were acquired with a charge-coupled device camera. Fluorescence intensity was determined either qualitatively by a blinded observer or quantitatively using Scion/ImageJ imaging software.[34] Corrected total cell fluorescence was integrated density after subtraction of background (area selected × mean background fluorescence).[35]

RNA isolation, generation of cDNA, and reverse transcription PCR

Larvae (3 dpf) were anesthetized in tricaine and biopsied as described[36] for genotyping. Larvae were maintained in RNAlater (Ambion) and 15 of each genotype pooled for RNA extraction. Total RNA was isolated using the Purelink RNA isolation kit (Ambion), and reverse transcribed with Superscript Synthesis (Invitrogen). cDNAs were amplified (MyiQ; Bio-Rad) using SYBR Green Master Mix (Applied Biosystems) at 95°C for 10 minutes, 40 cycles of 95°C for 30 seconds, 55°C for 30 seconds. Each was analyzed in triplicate and normalized to 18S ribosomal RNA, and expression presented as fold changes (ΔΔ cycle threshold [ΔΔCt]).[37]

Histologic examination

Humanely killed adult zebrafish were fixed in 4% buffered formalin overnight at room temperature, bisected in the midsagittal plane, embedded in paraffin, and sagittal sections produced at least 50 μm apart. Sections (3-4 μm) were hematoxylin and eosin stained.

Statistical analysis

Analyses were performed using χ^2, Mann-Whitney *U*, Fisher exact, or 2-tailed Student *t* tests. Log-rank testing of survival curves was performed using Prism (GraphPad Software). For statistical comparisons between individual transgenic rescue experiments, results from homozygous mutants were normalized to the median of their heterozygous clutchmates. *P* values

Table 1. Genotyping results of heterozygous incrosses from mutant line at3$^{\Delta 90}$

Line	Age	+/+	+/−	−/−	P (χ^2)
Δ90	12 dpf	18	49	23	0.53
	24 dpf	20	43	21	0.96
	2 mpf	55	94	24	0.002
	3 mpf	57	101	23	5.0E-04
	4 mpf	90	209	22	2.4E-13

were calculated with the Mann-Whitney U test by comparing the normalized data, followed by Bonferroni correction.

Results

Targeted disruption of *at3* using genome editing nucleases results in adult lethality in association with massive intracardiac thrombosis

We used OPEN[19,22,23] to produce 4 ZFN pairs designed to cleave exon 5 of the zebrafish *at3* genomic locus (zebrafish nomenclature guidelines dictate use of "*at3*" for the gene, "At3" for protein[38]). RNA encoding each ZFN pair was injected into the cytoplasm of single-cell embryos, with 1 pair producing somatic mutations (Figure 1A) at a frequency of 1.6% (3 of 192 sequenced clones from 2 pools of 8 embryos). The remaining embryos were raised to adulthood, and 46 of these F0 fish were mated to wild-type fish to confirm germline transmission. We identified 4 founders with the following mutations: 4-bp insertion (*at3*$^{+4}$), 6-bp deletion (*at3*$^{\Delta 6}$), 22-bp deletion (*at3*$^{\Delta 22}$), and 90-bp deletion (*at3*$^{\Delta 90}$) (Figure 1B). *at3*$^{+4}$, *at3*$^{\Delta 22}$, and *at3*$^{\Delta 90}$ produced frameshifts in exon 5 and are predicted to result in null alleles (the 90-bp deletion removes the splice donor site) (supplemental Table 3). *at3*$^{\Delta 22}$ and *at3*$^{\Delta 90}$ heterozygotes were incrossed, with similar results for both mutants. Genotyping between 2 and 24 dpf revealed the expected Mendelian distribution (Table 1) with no visible phenotypes. However, beginning at ~2 months postfertilization (mpf), we observed a significant loss of homozygotes (Table 1), with ~80% dying between 2 and 7 mpf (Figure 1C). Approximately 5% of *at3*$^{-/-}$ mutants had externally visible hemorrhage (Figure 1D). Reverse transcription PCR (RT-PCR) indicated reduction of *at3* expression in heterozygotes, and absence of expression in homozygous mutants, presumably due to nonsense-mediated decay[39] (Figure 1E-F).

To rule out potential off-target ZFN mutations, we injected *at3*$^{\Delta 22}$ incrosses with an *at3* cDNA under control of the zebrafish *ubiquitin* (*ubi*) promoter (*ubi-at3*)[26]. After 1 year, homozygotes displayed significantly greater survival compared with uninjected *at3*$^{-/-}$ fish (Figure 1G).

Histologic examination of surviving *at3*$^{-/-}$ fish at 2 to 3 mpf revealed large intracardiac thrombi in all homozygous mutants examined (n = 10), but not in wild-type (n = 10) or heterozygous mutants (n = 10) (Figure 2A-D). Notably, evaluation of a *ubi-at3* rescued homozygous *at3*$^{\Delta 22}$ mutant found no evidence of thrombosis at 16 mpf (supplemental Figure 3).

at3 homozygous mutants display an increased time to occlusion in an induced model of venous thrombosis

Complete deficiency of AT3 in mice and humans results in lethal thrombosis in utero.[1,5] Although loss of zebrafish At3 resulted in

apparently lethal thrombosis in adults, embryos and larvae appeared grossly normal with no overt evidence of pathologic thrombosis. We performed laser injury[14,17] at 3 to 4 dpf on larvae derived from *at3*$^{+/-}$ intercrosses, targeting the posterior cardinal vein (PCV) (orthologous to the mammalian inferior vena cava; supplemental Figure 4 and supplemental Video). As expected, wild-type and *at3*$^{+/-}$ larvae exhibited vessel occlusion within 2 minutes, but *at3*$^{-/-}$ mutants failed to occlude within that time period (Figure 3A). To confirm the role of At3 deficiency in this bleeding phenotype, we injected *ubi* regulated human and zebrafish *at3* cDNAs into single-cell embryos of wild-type and *at3*$^{-/-}$ clutchmates, followed by laser injury at 3 dpf. Fifty-two and 83% of human and zebrafish transgene-injected embryos, respectively, demonstrated a time to occlusion of <2 minutes ($P < .0001$ by the Mann-Whitney U test, Figure 3B-C).

The unexpected prolongation of clotting time in *at3*$^{-/-}$ larvae suggested the possibility of differential localization of zebrafish At3 compared with its mammalian ortholog. However, in situ hybridization at 5 dpf revealed strong mRNA expression localized predominantly to the liver, consistent with mouse and human AT3[40,41] (Figure 4A-D). Minor expression of *At3* has been noted in the notochord and neural tube of embryonic day 10.5 mice,[42] whereas early zebrafish embryos demonstrate weak yolk syncytial layer expression from 16 through 48 hours postfertilization.[43] Alignment with human AT3 revealed that the RCL was highly conserved across species (supplemental Figure 2). The orthologous P1 arginine was identified (Figure 4E), substituted with glycine (zebrafish Arg410Gly, orthologous to human Arg393), and assessed for binding to human thrombin in vitro (Figure 4F). Although wild-type At3 exhibited binding to thrombin and formed a putative thrombin-antithrombin complex, this interaction was absent in reactions with At3^{R410G} (Figure 4F). To prove that the mutant phenotype was dependent on known serine protease activity, an At3^{R410G} expressing cDNA was injected into *at3*$^{-/-}$ embryos. Consistent with the in vitro–binding studies, At3^{R410G} failed to rescue the *at3*$^{-/-}$ larval bleeding phenotype (Figure 4G). Taken together, these data strongly suggest that the observed *at3*$^{-/-}$ larval phenotype is due to loss of anticoagulant activity.
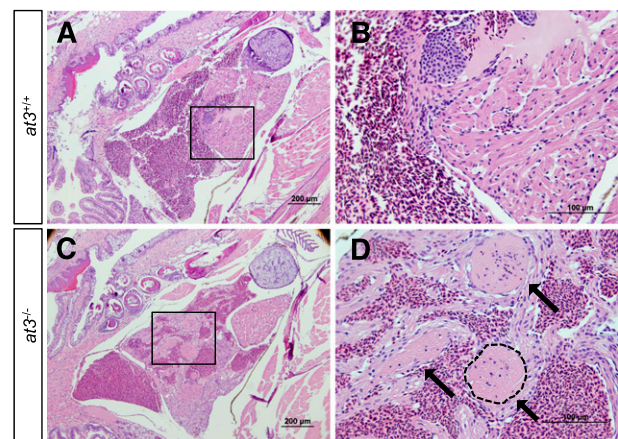

Figure 2. Loss of At3 results in adult intracardiac thrombosis. (A-D) *at3*$^{-/-}$ fish die in association with large intracardiac thrombi. H&E-stained cardiac sections from wild-type clutchmates (A-B) and *at3*$^{\Delta 90}$ homozygous mutants (C-D). The boxed regions in panels A and C are shown at higher magnification in panels B and D, respectively. Sections were photographed with an Olympus BX-51 upright light microscope using an Olympus DP-70 digital camera. Three large thrombi present in panels C and D are indicated by arrows in panel D. One thrombus is outlined. Scale bar 200 µm (A,C), 100 µm (B,D). H&E, hematoxylin and eosin.
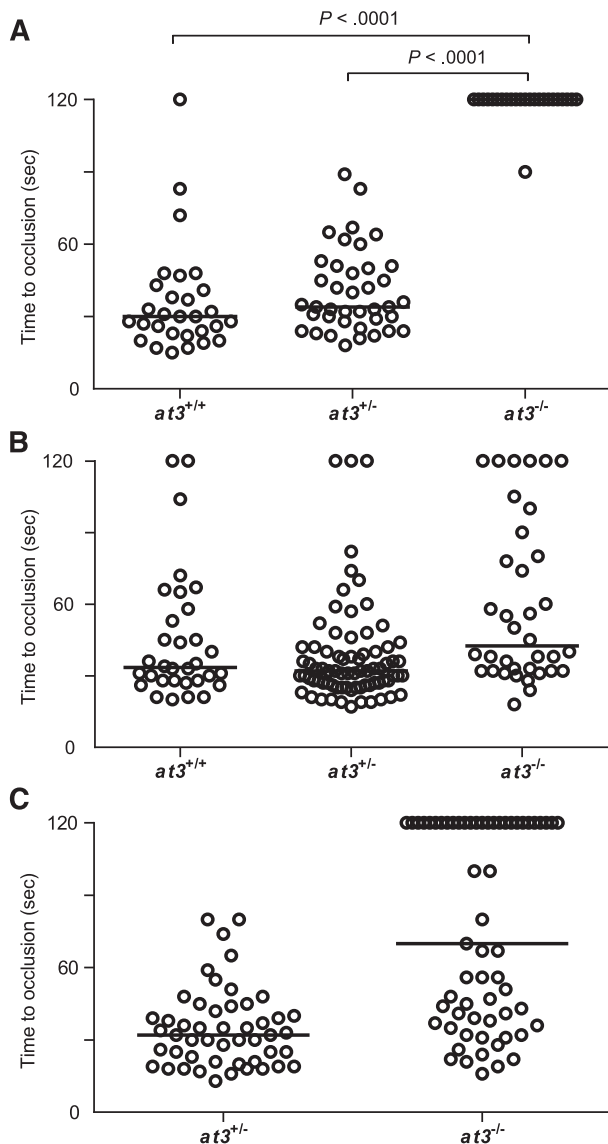
A

B

C

Figure 3. Loss of At3 prevents endothelial injury induced venous occlusion. The endothelium was targeted and injured at 3 dpf, and the time to occlusion measured in seconds with a maximum of 120. All data shown are from Δ90 mutants. (A) Time to occlusion of larvae derived from $at3^{+/-}$ incrosses at 3 dpf ($at3^{-/-}$, n = 16). Results were similar for $at3^{Δ22}$ mutants. (B) Time to occlusion of larvae (3 dpf) derived from $at3^{+/-}$ incross progeny injected at the 1-cell stage with the zebrafish $at3$ cDNA transgene ($at3^{-/-}$, n = 36) is significantly different from homozygotes in panel A, $P < .0001$. (C) Time to occlusion of larvae (3 dpf) derived from $at3^{+/-} \times at3^{-/-}$ progeny injected at the 1-cell stage with the human $at3$ cDNA transgene ($at3^{-/-}$, n = 61) is significantly different from homozygotes in panel A, $P < .0001$. Circles represent individual larvae. Data are from at least 3 independent experiments. Statistical significance was determined by the Mann-Whitney U test. Horizontal bars represent the median time to occlusion.

Hypofibrinogenemia in *at3* homozygous mutants explains the increased time to occlusion in larvae

To explain the paradoxical bleeding of $at3^{-/-}$ larvae, we hypothesized that loss of At3 function results in unregulated procoagulant activity, leading to consumption of fibrinogen, and lack of occlusion after endothelial injury. We infused activated bovine thrombin into larvae to evaluate relative concentrations of clottable fibrinogen at 3 to 4 dpf.[33] We observed a significant decrease in the number of larvae with severe vascular obstruction (9% of injected $at3^{-/-}$ vs 73% and 50% of $at3^{+/+}$ and $at3^{+/-}$, respectively) (Figure 5A), data

consistent with lower levels of fibrinogen in $at3^{-/-}$ mutants. Furthermore, quantification of fibrinogen antigen in adult plasma revealed a 68% decrease in $at3^{-/-}$ relative to $at3^{+/+}$ ($P < .05$, Figure 5B).

Examination of fibrinogen α (*fga*) and β (*fgb*) expression at 3 dpf demonstrated that there were no differences in mRNA accumulation (Figure 5C). Infusion with human fibrinogen prior to laser injury at 3 dpf rescued the bleeding phenotype in 52% of $at3^{-/-}$ larvae (Figure 5D, $P < .05$ by Mann-Whitney U test when compared with uninjected control). Treatment of larvae prior to laser injury with the fibrinolysis inhibitor ε-aminocaproic acid also rescued the $at3^{-/-}$ bleeding phenotype (Figure 5E, $P < .01$).

Hypofibrinogenemia in *at3⁻/⁻* mutants is secondary to DIC

We hypothesized that the mechanism underlying the discrepant adult thrombotic and larval bleeding phenotypes in *at3* mutants was DIC, with microscopic fibrin deposition. To identify the location of purported fibrin, human fibrinogen was labeled with FITC[44] and infused into $at3^{+/-}$ intercross progeny. Widespread PCV fluorescence was observed in *at3* homozygous mutant larvae after infusion, but absent in wild-type and heterozygous siblings (Figure 6A-E). Warfarin prevented laser-induced thrombosis in wild-type larvae (supplemental Figure 5), and pretreatment of $at3^{-/-}$ larvae eliminated fluorescence accumulation (Figure 6F). Coinjection of tPA partially prevented accumulation, as did postinjection (Figure 6G-H). Taken together, these data support the presence of DIC with consumption of fibrinogen in $at3^{-/-}$ mutants.

Evaluation of human *AT3* mutations in vivo

We examined several additional well-described human AT3 mutations associated with thrombosis, R393H,[45-49] A404D,[8] L99F,[50,51] K114E,[52,53] as well as a variant with greatly reduced anti-IXa and anti-Xa activity, Y253A[54] (Figure 7). The P1 arginine mutant R393H was unable to reverse the DIC in $at3^{-/-}$ larvae. Surprisingly, the RCL mutant A404D and heparin-binding mutants L99F and K114E all demonstrated significant rescue, although the former was less potent than the latter two. Human AT3 Y253A also reversed the bleeding phenotype and was significantly more efficient when compared with human AT3 ($P < .001$).

Discussion

We report targeted mutagenesis of zebrafish *at3* via ZFNs, one class of genome editing nucleases. Our data demonstrate that zebrafish survive complete loss of At3 with rampant DIC in the embryonic and larval periods, but apparently succumb to massive intracardiac thrombosis in adulthood. Concordant with our data, embryonic $At3^{-/-}$ mutant mice display a consumptive coagulopathy with secondary hemorrhage, although this causes in utero thrombosis and subsequent demise.[5] It is notable that in both the complete mouse knockout and a heparin-binding mutant knockin (Arg48Cys),[55] the heart is one of the most prominent sites of spontaneous thrombosis. The structure of the adult zebrafish heart has been described in detail,[56] and overall cardiovascular development is highly comparable to mammalian and avian species. Taken together, our data support the contention that although the timing of ultimate lethal thrombosis is different between zebrafish and mammals, the underlying mechanisms of the coagulation cascade are conserved.

Our studies indicate that loss of At3 leads to dysregulation of coagulation, resulting in consumption of fibrinogen and prolonged

Figure 4. Conservation of zebrafish At3 expression and function. (A-D) In situ hybridization for *at3* mRNA demonstrates liver-specific expression in 5 dpf larvae. Larvae were photographed with an Olympus BX-51 upright light microscope using an Olympus DP-70 digital camera. (A-B) Left lateral view at low and high magnification, respectively. (C-D) Dorsal view at low and high magnification, respectively. Arrow indicates the liver. Scale bar, 10 µm (C), 100 µm (D). In situ hybridization with a sense strand probe did not show any signal (not shown). (E) Alignment of the region flanking the AT3 P1 arginine (arrowhead). (F) Western blot analysis (using anti-human thrombin antibody) on recombinant At3 pulled down with human thrombin after expression in HEK 293 cells. Thrombin input only (−), pCDNA3.1 without insert (empty), pCDNA3.1z*at3* (At3), and pCDNA3.1z*at3*R410G (At3^R410G). The intermediate band present at ~50 kDa is an unknown protein present in the cell lysate and recognized by the antibody, but unrelated to expression of At3. (G) Time to occlusion of larvae (3 dpf) derived from *at3*^+/− × *at3*^−/− progeny injected at the 1-cell stage with the zebrafish At3^R410G expressing cDNA transgene regulated by the *ubi* promoter (*at3*^−/−, n = 34). Horizontal bars represent the median of time to occlusion.
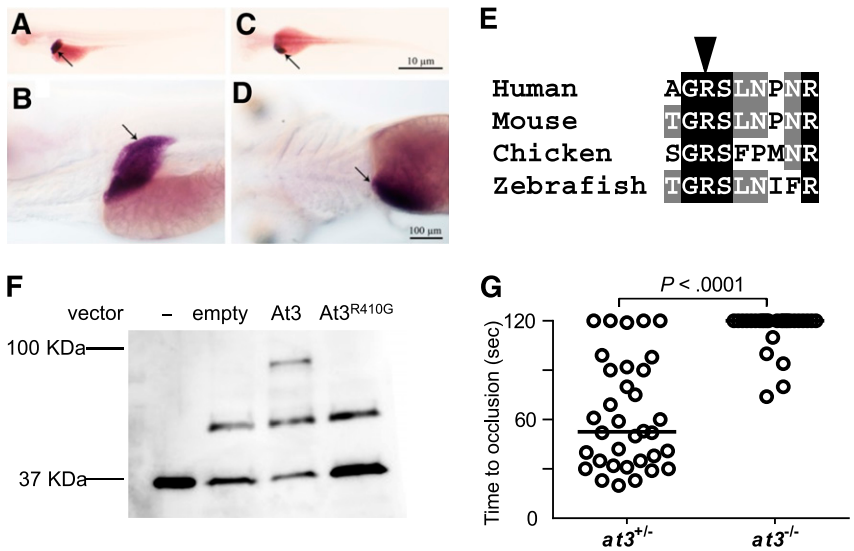
clotting times in *at3* homozygous mutant larvae. Although there were clearly visible spontaneous macrovascular thrombi in adult fish, injection of fluorescent fibrinogen identified disseminated microvascular thrombi in larvae, the latter consistent with clinical DIC. In patients, DIC is characterized by unregulated and excessive thrombin generation, resulting in fibrin formation with secondary plasminogen activation and fibrinolysis.[57] Clinical bleeding and/or thrombosis develops depending on the balance between thrombin and plasmin generation. In *at3*^−/− larvae, ε-aminocaproic acid, an inhibitor of plasmin, rescued the bleeding phenotype, demonstrating conservation of the fibrinolytic system. This also signifies possible contributions of fibrinolysis in this model, consistent with human DIC. These data demonstrate that loss of At3 results in unopposed procoagulant activity and possible secondary fibrinolytic activity, confirming a conserved role for zebrafish At3 as a key regulator of blood coagulation. Notably, extensive intracranial and subcutaneous hemorrhage was observed in
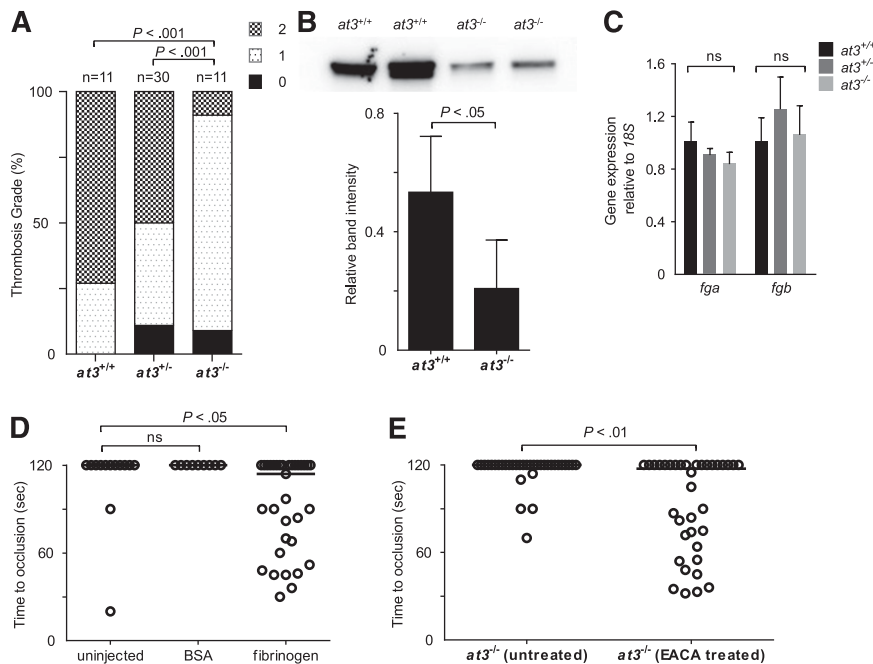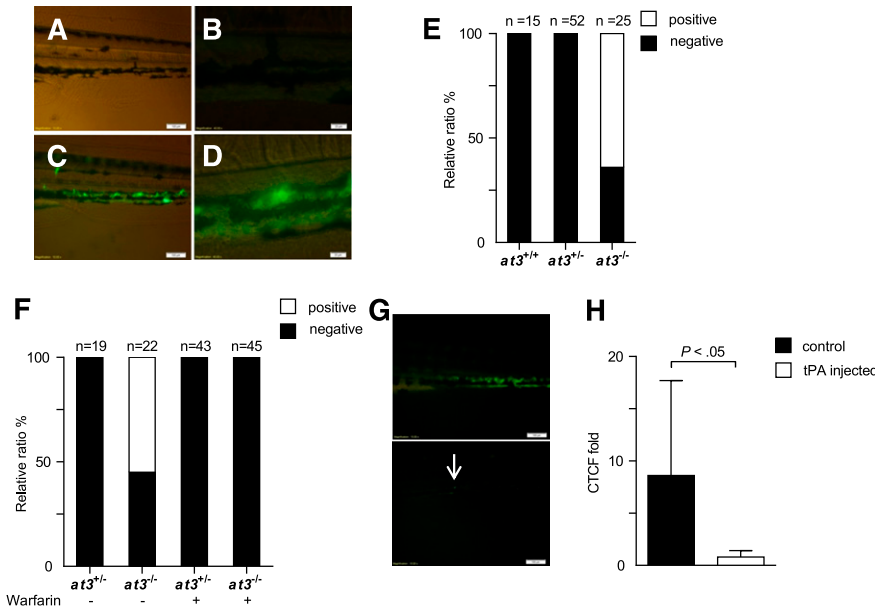

Figure 5. Evidence for fibrinogen consumption in *at3* homozygous mutant larvae and adults. All data shown are from Δ90 mutants. (A) Thrombin injection of larvae derived from *at3*^+/− incrosses at 4 dpf. Bar graph represents percentage of each thrombosis grade. Grade 0, normal flow within the PCV and dorsal aorta; grade 1, partial obstruction of flow in the PCV and dorsal aorta due to thrombus formation; grade 2, complete obstruction of flow. Statistical significance was determined by Fisher exact test. (B) Top: Western blot analysis of fibrinogen in adult plasma isolated from *at3*^+/+ and *at3*^−/− clutchmates. Bottom: Quantification of fibrinogen in plasma from *at3*^+/+ and *at3*^−/− clutchmates from 3 separate experiments, n = 4 per genotype. Error bars represent standard deviation and statistical significance was determined by a paired *t* test. (C) Quantitative real-time PCR demonstrates no significant difference of *fga* and *fgb* mRNA expression in *at3*^+/+ and *at3*^−/− clutchmates (3 dpf, n = 15 per genotype). Error bars represent standard deviation and statistical significance was determined by a paired *t* test. (D) Rescue of time to laser-induced occlusion by human fibrinogen injection at 3 dpf. *at3*^−/− mutant clutchmates were injected with human fibrinogen or BSA. Uninjected (n = 13), BSA injection (n = 9), and human fibrinogen injection (n = 33). (E) Effects of EACA (100 mM) pretreatment on *at3*^−/− larvae. Untreated (n = 34), EACA treated (n = 36). Circles represent individual larvae. Statistical significance was determined by the Mann-Whitney *U* test. Horizontal bars represent the median time to occlusion. BSA, bovine serum albumin; EACA, ε-aminocaproic acid; ns, nonsignificant.

Figure 6. *at3*^{−/−} mutants display fibrin deposition, consistent with DIC. Fluorescent deposits were observed in the PCV in *at3*^{−/−} mutant larvae after FITC-labeled fibrinogen injection. All data shown are from Δ90 mutants and were collected by an observer blinded to genotype and/or treatment. (A-B) Images of *at3*^{+/+} and (C-D) *at3*^{−/−} larvae postinjection. Scale bars: (A,C), 100 μm; (B,D), 20 μm. (E) Percentage of larvae identified without (black) or with fluorescent PCV deposits (white), derived from *at3*^{+/−} incrosses or *at3*^{+/−} × *at3*^{−/−}. Data are from 3 separate experiments. (F) Effects of warfarin pretreatment on *at3*^{−/−} larvae prior to FITC-labeled fibrinogen injection demonstrate that fluorescence deposition is inhibited by anticoagulation. (G) Effects of tPA on *at3*^{−/−} larvae post FITC-labeled fibrinogen injection. Presence of fluorescent venous deposits seen prior to injection of tPA (top) were significantly diminished post tPA injection (bottom). Scale bars: 100 μm. Arrow indicates minor residual fluorescence. (H) Quantification of CTCF of *at3*^{−/−} larvae post tPA injection. Control, n = 7; tPA injected, n = 6. Error bars represent standard deviation and statistical significance was determined by an unpaired *t* test. Larvae were visualized on an inverted microscope Olympus IX71 with 40× objective and images were acquired with a charge-coupled device camera (Olympus DP72, cellSens software 1.3). CTCF, corrected total cell fluorescence.

mouse *At3*^{−/−} embryos, without detectable accumulation of fibrinogen in those tissues.[5] The authors posited that a consumptive coagulopathy depleted fibrinogen from the plasma, resulting in the observed bleeding, as we discerned in *at3*^{−/−} mutants. Similarly, *Proc* knockout mice displayed intracranial hemorrhage in addition to thrombi in the heart and other organs, and clottable fibrinogen was undetectable.[2] Recently, *fga* was targeted in zebrafish using ZFNs, and the authors demonstrated complete absence of fibrinogen.[58] They did not observe specific bleeding in homozygous mutant larvae, but did note sporadic adult hemorrhage, both consistent with our data (Figure 1D). In contrast, they only detected a partial reduction in

survival of homozygous mutants, supporting our data that suggest *at3*^{−/−} mutants die of thrombosis rather than hemorrhage.

The observation that spontaneous, nonocclusive thrombosis due to DIC is so well tolerated in fish embryos and larvae raises important questions about the role of the coagulation system in vertebrate development. It is tempting to speculate that additional biological mechanisms may play a role, either through established clotting or other pathways. There may be protective species-specific factors for critical determinants of hemostatic balance, and the ability to perform high-throughput genetic screens in the zebrafish could lead to the identification of novel modifying factors.[18] Another powerful application for zebrafish is small-molecule screening, which has led to the rapid clinical development of a novel therapeutic approach for cord blood transplant.[59-61] Screens for novel anticoagulants or modulators of DIC might also have the potential to lead to innovative therapeutic modalities.

Alignment of human to zebrafish At3 reveals 55% identity and 70% similarity (supplemental Figure 2 and Kumar et al[62]). Because human AT3 rescued the prolonged time to occlusion in our endothelial injury assay, we performed semiquantitative evaluation of various human mutations and targeted substitutions. Substitution of the RCL P1 arginine (Arg393His) has been identified in several individuals and families with thrombophilia,[45-49] and has been shown to alter AT3 function in vitro.[63] Arg393His abolished AT3 activity, confirming the results of biochemical analysis as well as demonstrating the ability of this in vivo model to evaluate human coagulation factor variants. Ala404Asp, a substitution in the RCL with pleiotropic effects that alters interactions with both thrombin and heparin,[8] demonstrated statistically significant rescue, although the average time to occlusion was longer than wild-type AT3. Leu99Phe,[50,51] identified in patients with venous thromboembolism, demonstrated rescue consistent with wild-type AT3, as did another heparin-binding mutant Lys114Glu.[52,53] The fact that heparin binding appears disposable was surprising, but consistent with human clinical data. Although mutations that abolish protease inhibition are sufficient to increase thrombosis risk in the heterozygous state, heparin-binding site mutations only manifest in homozygotes.[64] Human Tyr253 is a critical residue of an AT3
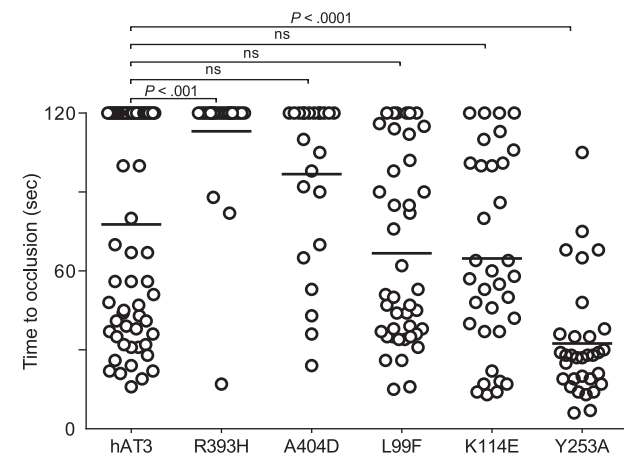

Figure 7. Effect of human AT3 substitutions in vivo. One-cell embryos were injected with individual wild-type or mutant human AT3 cDNAs, under regulation of the *ubi* promoter. At 3 dpf, the endothelium was targeted and the time to occlusion measured by a blinded observer. All larvae were derived from *at3*[+/Δ90] incrosses or *at3*[+/Δ90] × *at3*[Δ90/Δ90]. Data from *at3*[Δ90/Δ90] mutants injected with wild-type human AT3 cDNA were compared with *at3*[Δ90/Δ90] injected with mutant human AT3 cDNAs, R393H (*at3*[Δ90/Δ90], n = 25), A404D (*at3*[Δ90/Δ90], n = 23), L99F (*at3*[Δ90/Δ90], n = 42), K114E (*at3*[Δ90/Δ90], n = 14), Y253A (*at3*[Δ90/Δ90], n = 32). For statistical analysis, data were normalized to heterozygous clutchmates and significance determined by the Mann-Whitney *U* test followed by Bonferroni correction (see "Methods"). Horizontal bars represent the median of time to occlusion. ns, nonsignificant.

IXa- and Xa-binding exosite.[54] Surprisingly, AT3^{Tyr253Ala} rescued the $at3^{-/-}$ coagulopathy with a greater potency than wild type. Although only semiquantitative, these data suggest that proper hemostatic balance primarily depends on thrombin inhibition. Also, AT3^{Tyr253Ala} exhibits enhanced rates of thrombin inhibition in the presence of heparin,[54] which could explain the increased activity. Taken together, these data provide novel insights into AT3 function in vivo. Our approach establishes a rapid and robust new paradigm for validating human genetic variants associated with coagulation disorders, as well as complements biochemical and structure/function studies.

Acknowledgments

J.A.S. is the Diane and Larry Johnson Family Scholar of Pediatrics and Communicable Diseases.

Authorship

Contribution: Y.L. designed and performed research, analyzed data, and wrote the manuscript; C.A.K. designed and performed research, and analyzed data; M.L.M. and J.K.J. designed and performed research; C.E.R., P.T., M.C.H., A.H.V., T.R., and Z.H. performed research; R.M. analyzed data; S.T.O. designed research and analyzed data; and J.A.S. designed, performed, and supervised research, analyzed data, and wrote the manuscript.

Conflict-of-interest disclosure: J.K.J. has financial interests in Editas Medicine and Transposagen Biopharmaceuticals. J.K.J.'s interests were reviewed and are managed by Massachusetts General Hospital and Partners HealthCare in accordance with their conflict of interest policies. The remaining authors declare no competing financial interests.

The current affiliation for M.L.M. is Editas Medicine, Cambridge, MA. The current affiliation for A.H.V. is Graduate Program in Molecular Biosciences, University of Chicago, Chicago, IL.

Correspondence: Jordan Shavit, Department of Pediatrics, University of Michigan, Room 8301 Medical Science Research Building III, 1150 W Medical Center Dr, Ann Arbor, MI 48109-5646; e-mail: jshavit@umich.edu.

References

1. Shavit JA, Ginsburg D. Hemophilias and Other Disorders of Hemostasis. In: Rimoin DL, Pyeritz RE, Korf B, eds. *Emery and Rimoin's Principles and Practice of Medical Genetics.* 2013:1-33.

2. Jalbert LR, Rosen ED, Moons L, et al. Inactivation of the gene for anticoagulant protein C causes lethal perinatal consumptive coagulopathy in mice. *J Clin Invest.* 1998;102(8):1481-1488.

3. Burstyn-Cohen T, Heeb MJ, Lemke G. Lack of protein S in mice causes embryonic lethal coagulopathy and vascular dysgenesis. *J Clin Invest.* 2009;119(10):2942-2953.

4. Saller F, Brisset AC, Tchaikovski SN, et al. Generation and phenotypic analysis of protein S-deficient mice. *Blood.* 2009;114(11):2307-2314.

5. Ishiguro K, Kojima T, Kadomatsu K, et al. Complete antithrombin deficiency in mice results in embryonic lethality. *J Clin Invest.* 2000;106(7): 873-878.

6. Huntington JA. Serpin structure, function and dysfunction. *J Thromb Haemost.* 2011;9(suppl 1): 26-34.

7. Olson ST, Gettins PG. Regulation of proteases by protein inhibitors of the serpin superfamily. *Prog Mol Biol Transl Sci.* 2011;99:185-240.

8. Luxembourg B, Delev D, Geisen C, et al. Molecular basis of antithrombin deficiency. *Thromb Haemost.* 2011;105(4):635-646.

9. Hanumanthaiah R, Day K, Jagadeeswaran P. Comprehensive analysis of blood coagulation pathways in teleostei: evolution of coagulation factor genes and identification of zebrafish factor VIIi. *Blood Cells Mol Dis.* 2002;29(1):57-68.

10. Davidson CJ, Tuddenham EG, McVey JH. 450 million years of hemostasis. *J Thromb Haemost.* 2003;1(7):1487-1494.

11. Davidson CJ, Hirt RP, Lal K, et al. Molecular evolution of the vertebrate blood coagulation network. *Thromb Haemost.* 2003;89(3):420-428.

12. Jiang Y, Doolittle RF. The evolution of vertebrate blood coagulation as viewed from a comparison of puffer fish and sea squirt genomes. *Proc Natl Acad Sci USA.* 2003;100(13):7527-7532.

13. Fish RJ, Vorjohann S, Béna F, Fort A, Neerman-Arbez M. Developmental expression and organisation of fibrinogen genes in the zebrafish. *Thromb Haemost.* 2012;107(1):158-166.

14. Vo AH, Swaroop A, Liu Y, Norris ZG, Shavit JA. Loss of fibrinogen in zebrafish results in symptoms consistent with human hypofibrinogenemia. *PLoS ONE.* 2013;8(9): e74682.

15. Carrillo M, Kim S, Rajpurohit SK, Kulkarni V, Jagadeeswaran P. Zebrafish von Willebrand factor. *Blood Cells Mol Dis.* 2010;45(4):326-333.

16. Ghosh A, Vo A, Twiss BK, et al. Characterization of zebrafish von Willebrand factor reveals conservation of domain structure, multimerization, and intracellular storage. *Adv Hematol.* 2012; 2012:214209.

17. Jagadeeswaran P, Carrillo M, Radhakrishnan UP, Rajpurohit SK, Kim S. Laser-induced thrombosis in zebrafish. *Methods Cell Biol.* 2011;101: 197-203.

18. Santoriello C, Zon LI. Hooked! Modeling human disease in zebrafish. *J Clin Invest.* 2012;122(7): 2337-2343.

19. Foley JE, Yeh JR, Maeder ML, et al. Rapid mutation of endogenous zebrafish genes using zinc finger nucleases made by Oligomerized Pool ENgineering (OPEN). *PLoS ONE.* 2009;4(2): e4348.

20. Sander JD, Cade L, Khayter C, et al. Targeted gene disruption in somatic zebrafish cells using engineered TALENs. *Nat Biotechnol.* 2011;29(8): 697-698.

21. Hwang WY, Fu Y, Reyon D, et al. Efficient genome editing in zebrafish using a CRISPR-Cas system. *Nat Biotechnol.* 2013;31(3):227-229.

22. Maeder ML, Thibodeau-Beganny S, Osiak A, et al. Rapid "open-source" engineering of customized zinc-finger nucleases for highly efficient gene modification. *Mol Cell.* 2008;31(2): 294-301.

23. Maeder ML, Thibodeau-Beganny S, Sander JD, Voytas DF, Joung JK. Oligomerized pool engineering (OPEN): an 'open-source' protocol for making customized zinc-finger arrays. *Nat Protoc.* 2009;4(10):1471-1501.

24. Foley JE, Maeder ML, Pearlberg J, Joung JK, Peterson RT, Yeh JR. Targeted mutagenesis in zebrafish using customized zinc-finger nucleases. *Nat Protoc.* 2009;4(12):1855-1867.

25. Rozen S, Skaletsky H. Primer3 on the WWW for general users and for biologist programmers. *Methods Mol Biol.* 2000;132:365-386.

26. Mosimann C, Kaufman CK, Li P, Pugach EK, Tamplin OJ, Zon LI. Ubiquitous transgene expression and Cre-based recombination driven by the ubiquitin promoter in zebrafish. *Development.* 2011;138(1):169-177.

27. Li MZ, Elledge SJ. SLIC: a method for sequence- and ligation-independent cloning. *Methods Mol Biol.* 2012;852:51-59.

28. Zheng L, Baumann U, Reymond JL. An efficient one-step site-directed and site-saturation mutagenesis protocol. *Nucleic Acids Res.* 2004; 32(14):e115.

29. Kawakami K, Takeda H, Kawakami N, Kobayashi M, Matsuda N, Mishina M. A transposon-mediated gene trap approach identifies developmentally regulated genes in zebrafish. *Dev Cell.* 2004;7(1):133-144.

30. Jagadeeswaran P, Sheehan JP. Analysis of blood coagulation in the zebrafish. *Blood Cells Mol Dis.* 1999;25(3-4):239-249.

31. Pedroso GL, Hammes TO, Escobar TD, Fracasso LB, Forgiarini LF, da Silveira TR. Blood collection

for biochemical analysis in adult zebrafish. *J Vis Exp.* 2012;(63):e3865.

32. Thisse C, Thisse B. High-resolution in situ hybridization to whole-mount zebrafish embryos. *Nat Protoc.* 2008;3(1):59-69.

33. Kalish Y, Ghosh A, Shavit JA, Ginsburg D. Conservation of hemostatic system component function between zebrafish and mammals. *Blood.* 2009;114(22):1228-1229.

34. Schneider CA, Rasband WS, Eliceiri KW. NIH Image to ImageJ: 25 years of image analysis. *Nat Methods.* 2012;9(7):671-675.

35. Cappell KM, Sinnott R, Taus P, Maxfield K, Scarbrough M, Whitehurst AW. Multiple cancer testis antigens function to support tumor cell mitotic fidelity. *Mol Cell Biol.* 2012;32(20): 4131-4140.

36. Wilkinson RN, Elworthy S, Ingham PW, van Eeden FJ. A method for high-throughput PCR-based genotyping of larval zebrafish tail biopsies. *Biotechniques.* 2013;55(6):314-316.

37. Pfaffl MW. A new mathematical model for relative quantification in real-time RT-PCR. *Nucleic Acids Res.* 2001;29(9):e45.

38. Wood R. *Genetic nomenclature Guide: With Information on Websites.* 1998th ed. Cambridge, UK: Elsevier Trends Journals; 1998.

39. Kervestin S, Jacobson A. NMD: a multifaceted response to premature translational termination. *Nat Rev Mol Cell Biol.* 2012;13(11):700-712.

40. Patnaik MM, Moll S. Inherited antithrombin deficiency: a review. *Haemophilia.* 2008;14(6): 1229-1239.

41. Diez-Roux G, Banfi S, Sultan M, et al. A high-resolution anatomical atlas of the transcriptome in the mouse embryo. *PLoS Biol.* 2011;9(1): e1000582.

42. Capellini TD, Dunn MP, Passamaneck YJ, Selleri L, Di Gregorio A. Conservation of notochord gene expression across chordates: insights from the Leprecan gene family. *Genesis.* 2008;46(11): 683-696.

43. Thisse C, Thisse B. High throughput expression analysis of ZF-models consortium clones. ZFIN direct data submission. 2005. http://zfin.org.

44. Gregory M, Hanumanthaiah R, Jagadeeswaran P. Genetic analysis of hemostasis and thrombosis

using vascular occlusion. *Blood Cells Mol Dis.* 2002;29(3):286-295.

45. Bauer KA, Ashenhurst JB, Chediak J, Rosenberg RD. Antithrombin "Chicago": a functionally abnormal molecule with increased heparin affinity causing familial thrombophilia. *Blood.* 1983;62(6): 1242-1250.

46. Owen MC, Beresford CH, Carrell RW. Antithrombin Glasgow, 393 Arg to His: a P1 reactive site variant with increased heparin affinity but no thrombin inhibitory activity. *FEBS Lett.* 1988;231(2):317-320.

47. Erdjument H, Lane DA, Panico M, Di Marzo V, Morris HR. Single amino acid substitutions in the reactive site of antithrombin leading to thrombosis. Congenital substitution of arginine 393 to cysteine in antithrombin Northwick Park and to histidine in antithrombin Glasgow. *J Biol Chem.* 1988;263(12):5589-5593.

48. Erdjument H, Lane DA, Panico M, et al. Antithrombin Chicago, amino acid substitution of arginine 393 to histidine. *Thromb Res.* 1989; 54(6):613-619.

49. Lane DA, Erdjument H, Flynn A, et al. Antithrombin Sheffield: amino acid substitution at the reactive site (Arg393 to His) causing thrombosis. *Br J Haematol.* 1989;71(1):91-96.

50. Olds RJ, Lane DA, Boisclair M, Sas G, Bock SC, Thein SL. Antithrombin Budapest 3. An antithrombin variant with reduced heparin affinity resulting from the substitution L99F. *FEBS Lett.* 1992;300(3):241-246.

51. Kuhle S, Lane DA, Jochmanns K, et al. Homozygous antithrombin deficiency type II (99 Leu to Phe mutation) and childhood thromboembolism. *Thromb Haemost.* 2001;86(4): 1007-1011.

52. Mushunje A, Zhou A, Huntington JA, Conard J, Carrell RW. Antithrombin 'DREUX' (Lys 114Glu): a variant with complete loss of heparin affinity. *Thromb Haemost.* 2002;88(3):436-443.

53. Picard V, Susen S, Bellucci S, Aiach M, Alhenc-Gelas M. Two new antithrombin variants support a role for K114 and R13 in heparin binding. *J Thromb Haemost.* 2003;1(2):386-387.

54. Izaguirre G, Olson ST. Residues Tyr253 and Glu255 in strand 3 of beta-sheet C of antithrombin are key determinants of an exosite made

accessible by heparin activation to promote rapid inhibition of factors Xa and IXa. *J Biol Chem.* 2006;281(19):13424-13432.

55. Dewerchin M, Hérault JP, Wallays G, et al. Life-threatening thrombosis in mice with targeted Arg48-to-Cys mutation of the heparin-binding domain of antithrombin. *Circ Res.* 2003;93(11): 1120-1126.

56. Hu N, Yost HJ, Clark EB. Cardiac morphology and blood pressure in the adult zebrafish. *Anat Rec.* 2001;264(1):1-12.

57. Liebman HA, Weitz IC. Disseminated intravascular coagulation. In: Hoffman R, Benz EJ, Shattil SJ, Furie B, Cohen HJ, McGlave P, eds. *Hoffman Hematology: Basic Principles and Practice.* Philadelphia, PA: Churchill Livingstone; 2005.

58. Fish RJ, Di Sanza C, Neerman-Arbez M. Targeted mutation of zebrafish fga models human congenital afibrinogenemia. *Blood.* 2014;123(14): 2278-2281.

59. North TE, Goessling W, Walkley CR, et al. Prostaglandin E2 regulates vertebrate haematopoietic stem cell homeostasis. *Nature.* 2007;447(7147):1007-1011.

60. Goessling W, Allen RS, Guan X, et al. Prostaglandin E2 enhances human cord blood stem cell xenotransplants and shows long-term safety in preclinical nonhuman primate transplant models. *Cell Stem Cell.* 2011;8(4):445-458.

61. Cutler C, Multani P, Robbins D, et al. Prostaglandin-modulated umbilical cord blood hematopoietic stem cell transplantation. *Blood.* 2013;122(17):3074-3081.

62. Kumar A, Bhandari A, Sarde SJ, Goswami C. Sequence, phylogenetic and variant analyses of antithrombin III. *Biochem Biophys Res Commun.* 2013;440(4):714-724.

63. Chuang YJ, Swanson R, Raja SM, Bock SC, Olson ST. The antithrombin P1 residue is important for target proteinase specificity but not for heparin activation of the serpin. Characterization of P1 antithrombin variants with altered proteinase specificity but normal heparin activation. *Biochemistry.* 2001;40(22):6670-6679.

64. van Boven HH, Lane DA. Antithrombin and its inherited deficiency states. *Semin Hematol.* 1997; 34(3):188-204.